Vol. 29 (1998) *ACTA PHYSICA POLONICA B* No 11

ELECTROPRODUCTION OF MESONS IN THE FIRST RESONANCE REGION*

R.W. Gothe, D. Wacker and B. Schoch

Universität Bonn, D-53115 Bonn, Germany

(Received July 9, 1998)

An experimental programme has been carried out at ELSA (ELectron Stretcher Accelerator) to investigate the four momentum transfer dependence of the N to Δ transition. In a series of electron scattering coincidence experiments on ^{1}H and ^{2}D the $-K^2$-range from $0.04\,\mathrm{GeV}^2/c^2$ to $0.8\,\mathrm{GeV}^2/c^2$ was sampled by measuring the ϑ_N^* and φ_N^* angular distributions of the double differential pion production cross sections. The so-determined ratio of the structure functions $R_{\mathrm{LT}}/R_{\mathrm{TT}}$ at a $-K^2=0.2\,\mathrm{GeV}^2/c^2$ is one of the first results obtained with the ELAN (Electron scattering collaboration at Bonn) time-of-flight spectrometer.

PACS numbers: 13.60.Le, 13.40.-f, 23.20.En, 23.20.Gq

1. Introduction

In contrast to the measured positive quadrupole moment and the corresponding prolate deformation of the deuteron, caused by tensor forces in the N–N-interaction leading to a d-state admixture to the ground state wave function, tensor forces between quarks in the nucleon can only lead to intrinsic deformations. Such intrinsic deformations cannot be measured directly if the spin as in the case of the nucleon is smaller than one, but in analogy to nuclear physics they become visible in ground state to excited state transitions. The electromagnetic $\Delta_{33}(1232)$-excitation of the nucleon is such a transition from the nucleon ground state to its first excited state, which is strongly dominated by the magnetic dipole ($M1$ *i.e.* M_{1+}) absorption. But angular momentum and parity conservation also allow quadrupole amplitude contributions, these are in the case of real photons only electric transverse quadrupole ($E2$ *i.e.* E_{1+}) and in the case of virtual photons additional electric longitudinal ($L2$ *i.e.* L_{1+}) or scalar ($C2$ *i.e.* S_{1+}) quadrupole

* Presented at the Meson'98 and Conference on the Structure of Meson, Baryon and Nuclei, Cracow, Poland, May 26–June 2, 1998.

amplitudes respectively, where both of them are strictly related by Coulomb gauge invariance. These quadrupole transition amplitudes are observables which are sensitive to possible deformations of the nucleon and/or the Δ. Many conceptionally different theoretical approaches try to refine the understanding and notion of the nucleon structure and subsequently of such deformations. Several of them attempt successfully to describe the electric quadrupole to magnetic dipole ratio (EMR) at the $K^2 = 0\,\mathrm{GeV}^2/c^2$ point of $-2.5\,\% \pm 0.2\,\% \pm 0.2\,\%$ as measured with real photons at MAMI (MAinzer MIkrotron) [1] or the similar result of $-3.0\,\% \pm 0.3\,\% \pm 0.2\,\%$ from LEGS (Laser Electron Gamma Source at Brookhaven National Laboratory) [2]. The $-K^2$-dependence of the quadrupole contributions to the $N \rightarrow \Delta$ transition reflects the radial distribution of the quadrupole transition densities and should therefore restrict the flexibility of the theoretical models even further.

The partial linear polarization of the exchanged virtual photon can be explored by detecting either the recoil nucleon or the produced pion out of the electron scattering plane. In several first generation out of plane experiments [3–6] the quadrupole amplitude S_{1+} has been extracted relative to the dominant magnetic dipole amplitude M_{1+}. It was realized that, out of the many contributions [7] from the different s- and p-wave amplitudes to the cross section, the ratio $\sqrt{2\varepsilon_{\mathrm{L}}(\varepsilon+1)}R_{\mathrm{LT}}/\varepsilon R_{\mathrm{TT}}$ is very sensitive to the scalar quadrupole to magnetic dipole ratio (SMR). Results of dynamical model calculations [8] quantitatively support this sensitivity to the S_{1+} and M_{1+} multipoles. The above mentioned experiments explored the momentum transfer region $-K^2 \geq 0.3$ $(\mathrm{GeV}/c)^2$ and found a rather flat behaviour of the SMR, see Fig. 4. A multipole analysis [9] of the very early data on electro-production [10] indicates that the absolute value of this ratio may increase by up to a factor of two in the momentum transfer range of $-K^2 < 0.3$ $(\mathrm{GeV}/c)^2$. In a dedicated recent experiment the neutral pion was measured with a $\vec{k}$-symmetric lead glass spectrometer of full φ_π-acceptance for asymmetric decaying pions at small polar angles and indeed at $-K^2 = 0.127\,\mathrm{GeV}^2/c^2$ a large SMR of $-12.7\,\% \pm 1.5\,\%$ was extracted [11], see Fig. 4.

2. Method and set-up

The differential electro-production cross section in the single-photon-exchange approximation factorizes in two parts. One describes the electron–photon vertex and the other the photon–nucleon vertex

$$\frac{d^5\sigma}{dE_{e'}\,d\Omega^*_\pi\,d\Omega_{e'}} = \Gamma_t \cdot \frac{d^2\sigma_v}{d\Omega^*_\pi}\,. \tag{1}$$

The leptonic vertex factor Γ_t represents the virtual photon flux for a given incoming and scattered electron momentum and the differential absorption cross section for the exchanged virtual photon. In the center-of-mass frame of the hadronic final state (CMS) the coincidence cross section for unpolarized electrons and an unpolarized target but polarized photons can be expressed as [12]

$$\frac{d^2\sigma_v}{d\Omega_\pi^*} = \frac{|\vec{q}^*|}{k_\gamma^*}\left(R_{\rm T} + \varepsilon_{\rm L} R_{\rm L} + \sqrt{2\varepsilon_{\rm L}(\varepsilon+1)}R_{\rm LT}\cos\varphi_\pi^* + \varepsilon R_{\rm TT}\cos 2\varphi_\pi^*\right), \quad (2)$$

where $|\vec{p}_2^*| = |\vec{q}^*|$ denotes the magnitude of the nucleon or pion momentum respectively, k_γ^* the equivalent energy required for a real photon in the CMS to excite the hadronic system and $R_{\rm T}$, $R_{\rm L}$, $R_{\rm LT}$, $R_{\rm TT}$ the transverse, longitudinal, transverse-longitudinal- and transverse-transverse-interference response functions reflecting the specific sensitivities of the cross section due to the polarization of the virtual photon with the appropriate polarization parameters ε and $\varepsilon_{\rm L}$, see also Fig. 1.

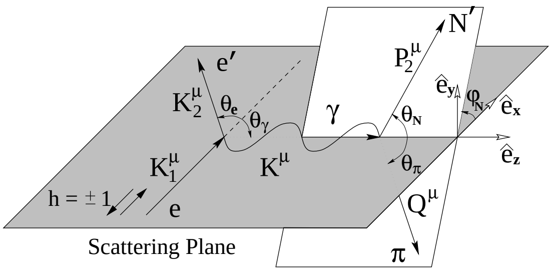

Fig. 1. Kinematics of the π-electro-production.

If the multipole analysis is restricted to s- and p-waves, the decomposition of the response functions yields on top of the $\Delta_{33}(1232)$-resonance, where the imaginary part of the magnetic dipole amplitude M_{1+} is close to its maximum and the real part vanishes, the highest sensitivity to the resonant multipole amplitudes M_{1+}, S_{1+} and E_{1+}. The strength of the scalar quadrupole amplitude S_{1+}, which is magnified in the case of $R_{\rm LT}$ by the interference with the dominant magnetic dipole amplitude M_{1+}, can be extracted relative to $R_{\rm TT}$ which is dominated by $|M_{1+}|^2$ out of the φ-modulation using a three-parameter-fit

$$\frac{d^2\sigma_v}{d\Omega_\pi^*} = A + B\cdot\cos\varphi_\pi + C\cdot\cos 2\varphi_\pi, \quad (3)$$

where $\frac{Re(S_{1+}^* M_{1+})}{|M_{1+}|^2}$, the SMR, is then directly proportional to $\frac{B}{C}$.

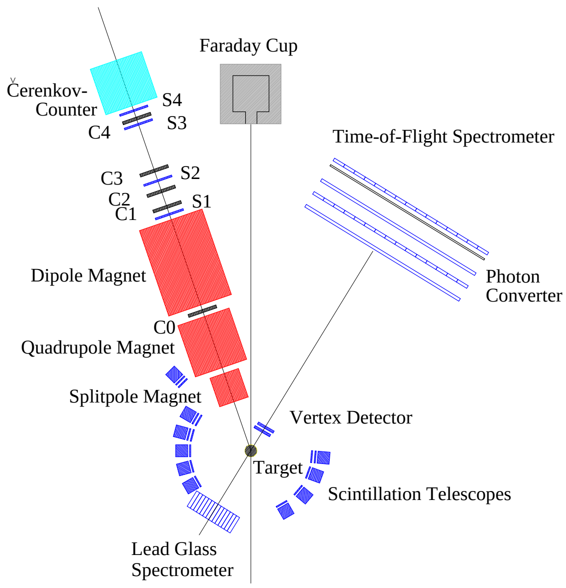

Fig. 2. Schematic experimental set-up.

The sketched experimental set-up, see Fig. 2, shows the electron beam, that penetrates a 6 cm long cylindrical target cell either filled with liquid hydrogen or deuterium and is caught by the Faraday cup to determine its current. The scattered electrons are analyzed in a magnetic spectrometer that comprises a dipole magnet as the dispersive element and two focusing quadrupole magnets. The electrons are traced by five multi-wire proportional chambers (C0-C4) and timed by a fourfold coincidence of the scintillation paddles (S1-S4). For the separation of heavier particles, like pions and muons, a Čerenkov counter is used. In order to fully exploit the azimuthal angle dependence of the differential cross section as given in Eq. (2) and the polar angle dependence of the response functions as disentangled by a multipole decomposition as in [12] a new time-of-flight (TOF) spectrometer was designed, optimized and built to detect protons, neutrons, charged pions and even photons in coincidence with the scattered electrons over the whole azimuthal ($0 \leq \varphi \leq 2\pi$) and a wide polar angle range. It consists of four time-of-flight walls, each has a surface of $3 \star 3\,\mathrm{m}^2$ and comprises 15 scintillation bars, which are 3 m long, 20 cm high and 5 cm thick. The correlated signals of the photomultiplier tubes at both ends of each bar provide the particle time-of-flight via the TDC (Time to Digital Converter) sum and the location of the detected particle via the TDC difference. The scintillation bars of each TOF wall are crossed with respect to those of the neighbouring walls generating a pattern of 225 segments of $20 \star 20\,\text{cm}^2$. This spatial resolution is further refined by the timing resolution of the TOF spectrometer, which is better than 300 ps (FWHM — Full Width at Half Maximum) corresponding to less than 5 cm (FWHM). Further resolutions depend also on the kinematics of the detected particle and are at a $-K^2 = 0.2\,\text{GeV}^2/c^2$ for the presented results typically smaller than 0.7^o (FWHM) for the polar angle in the laboratory frame (LAB) or 2.3^o (FWHM) in the CMS respectively and smaller than 1.5 % (FWHM) for the relative momentum $\frac{\Delta p}{p}$. The other components of the experimental set-up, see Fig. 2, as the vertex detector to increase the reliability of the neutron identification, the lead glass spectrometer to separate the $n\pi^0$ from the $p\pi^0$ channel and to see the virtual Compton scattering process at backward angles as well as the scintillation telescopes to measure the pionless deuteron break-up and to determine the neutron efficiency of the TOF spectrometer were not only needed to carry out the full experimental programme [13] but will also enable numerous consistency checks enhancing the reliability of further analyses.

3. First results

The $p(e,e'p')\pi^0$ experiment at $-K^2 = 0.2\,\text{GeV}^2/c^2$ covers an invariant mass range of $W = (1.232 \pm 0.070)\,\text{GeV}$ and was performed at ELSA that delivered an extracted electron beam with an energy of 1.6 GeV, an average current of $12\,nA$ and an average duty factor of 42 %. The magnetic spectrometer was set to an electron scattering angle of 18.95^o and a nominal momentum of $1.156\,\text{GeV}/c$ covering an acceptance of $\pm 140\,\text{MeV}$ with a resolution of 5 MeV (FWHM).

The φ^*- and ϑ^*-dependence of the $\vec{k}$-corrected proton distribution is analyzed in a $\pm 20\,\text{MeV}$ bin centered with respect to the $\Delta_{33}(1232)$-resonance. For $\vartheta^*_p < 50^o$ the φ-modulation is fitted according to Eq. (3) and plotted in Fig. 3. The fit parameters A, B and C are proportional to $R_T + \varepsilon_L R_L$, R_{LT} and R_{TT}, so that the SMR can be extracted from the ratio $\frac{B}{C}$ according to

$$\frac{Re(S^*_{1+}M_{1+})}{|M_{1+}|^2} = \frac{|\vec{k}^*|}{k^*_0} \cdot \frac{-1.5 \cdot \varepsilon \cdot \tan\vartheta^*_\pi}{6 \cdot \sqrt{2\varepsilon_L(\varepsilon+1)}} \cdot \frac{B}{C}\,. \tag{4}$$

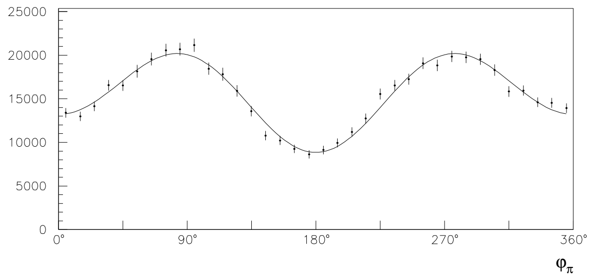

Fig. 3. Fit to the φ_π-modulation for $\vartheta_p^* < 50^o$.

4. Conclusion and outlook

Fig. 4 shows the recent [11] and the first new [14] SMR at the Δ_{33}-resonance together with the results of the previous measurements. The contribution of the S_{1+}-amplitude increases in the absolute magnitude relative to the M_{1+}-amplitude for smaller momentum transfers indicating a different spatial distribution of the transition densities for the electric longitudinal quadrupole and magnetic dipole transitions, respectively. The ongoing analysis of the accumulated data will improve the accuracy of the results and extend the momentum transfer range to both lower and higher values as marked in Fig. 4. In addition, the measurements of the $n\pi^+$-channel as well as the measurements on the deuteron will allow a precise separation of the different isospin channels.

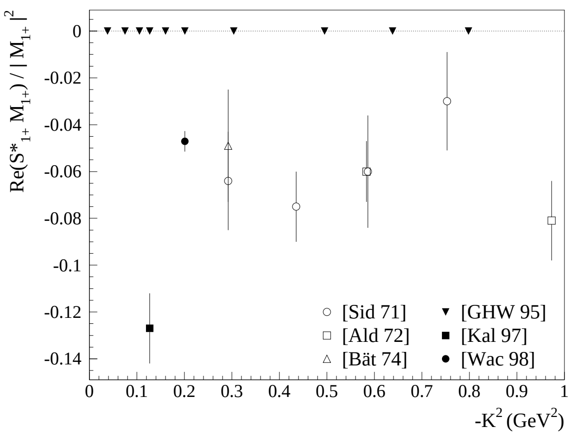

Fig. 4. $-K^2$-dependence of the $\frac{Re(S^*_{1+}M_{1+})}{|M_{1+}|^2}$ ratio and the marked $-K^2$ points of the proposed and completed ELAN experiment [13].

The authors thank the ELAN collaboration and the staff of ELSA for the physical and the Bundesministerium für Forschung und Technologie (06BN663/1) as well as the Deutsche ForschungsGemeinschaft, Schwerpunkt "Untersuchung der hadronischen Struktur von Nukleonen und Kernen mit elektromagnetischen Sonden", SCHO 226/5-1 for the financial support.

REFERENCES

[1] R. Beck *et al.*, *Phys. Rev. Lett.* **78**, 606 (1997).

[2] G. Blanpied *et al.*, *Phys. Rev. Lett.* **79**, 4337 (1997).

[3] W. Albrecht *et al.*, *Nucl. Phys.* **B27**, 615 (1971).

[4] R. Siddle *et al.*, *Nucl. Phys.* **B35**, 93 (1971).

[5] J.C. Alder *et al.*, *Nucl. Phys.* **B46**, 573 (1972).

[6] K. Bätzner *et al.*, *Nucl. Phys.* **B76**, 1 (1974).

[7] R.W. Lourie, *Phys. Rev.* **C45**, 540 (1992).

[8] P. Christillin *et al.*, *J. Phys. G: Nucl. Part. Phys.* **15**, 967 (1989); *J. Phys. G: Nucl. Part. Phys.* **16**, 805 (1990); *J. Phys. G: Nucl. Part. Phys.* **18**, 1915 (1992); *J. Phys. G: Nucl. Part. Phys.* **20**, 1169 (1994).

[9] R.L. Crawford *et al.*, *Nucl. Phys.* **B28**, 573 (1971).

[10] C. Mistretta *et al.*, *Phys. Rev.* **184**, 1487 (1969).

[11] F. Kalleicher *et al.*, *Z. Phys.* **A359**, 201 (1997).

[12] D. Drechsel *et al.*, *J. Phys. G: Nucl. Part. Phys.* **18**, 449 (1992).

[13] R.W. Gothe *et al.*, Proposal, Bonn (1995).

[14] D. Wacker, Dissertation, Bonn (1998).